ANALYSIS OF INFLUENCE OF THE LOAD PLANE COMBINED WITH PRELOAD ON DURABILITY OF BEARING

Jaroslaw Kaczor

Institute of Sanitary Engineering and Building Installations, Technical University of Lodz, Lodz, Poland

*E-mail of corresponding author: jaroslaw.kaczor@p.lodz.pl

Resume

Angular ball bearings are commonly used whenever there is a demand to increase stiffness of a bearing. The aforementioned increase of stiffness can be achieved by obtaining proper preload in bearings. In common belief, preload has a negative consequence: it increases the load of rolling elements, which must lead to lower durability of bearing compared to the situation before the preload use.

The objective of the research was to analyse how a change of load plane, while applying the preload, affects durability of angular ball bearings. In calculations of durability of bearings, besides elasticity of a shaft, radial, axial and bending elasticities of bearings were taken into consideration, as well.

Article info

Received 27 October 2021
Accepted 2 February 2022
Online 5 April 2022

Keywords:

angular ball bearings
preload
durability of bearing
bearing life

Available online: https://doi.org/10.26552/com.C.2022.3.B170-B188

ISSN 1335-4205 (print version)
ISSN 2585-7878 (online version)

1 Introduction

In modern scientific literature there can be found a lot of information concerning the effect of preload on bearings and bearing systems. The preload is applied not only in the case of angular contact ball bearings but also in the case of other bearings; e.g. [1] presents a generalization of previous works developed by the authors in the field of calculation and selection of slewing bearings where a theoretical model for estimation of the static load-carrying capacity of four-contact-point slewing bearings was obtained.

Authors of [2] present the results of experimental studies on the effects of mechanical preload and bearing clearance on the rotor dynamic performance of lobed gas foil bearings (GFBs) for oil-free turbochargers (TCs).

Great attention was paid to the effect of the preload on stiffness of machine tool spindles in relation to thermal effects; e.g. [3] presents a unified method to predict nonlinear thermal characteristics of a high-speed spindle bearing subjected to a preload. Based on the quasi-static model and finite difference method the change of thermal contact resistance, bearing parameters and heat source with temperature per second is completely analyzed using a new algorithm. As a result, the thermal effects on contact angles, contact forces, the preload and stiffness of the bearing are found. Moreover, analysis results show that the estimated preload and bearing stiffness nonlinearly vary with the increase in temperature. In [4], a multi-criteria optimization was performed for systems bearing-spindle. Many objectives were considered in this work, including vibration frequencies, static stiffness and total friction torque. Bearing preload and bearing position were selected as variable factors.

Then, in [5] are presented the effects of the preload and preload method on the rotational performance of the spindle-bearing system is explored experimentally to reveal the role of preload and preload method in spindle rotational performances under different speeds.

The angular contact ball bearing preload is very important for the high-speed spindles and has a very large effect on the dynamic and thermal characteristics of the spindles [6], vibrations [7], the performance of the spindle system and bearings in a machine tool [8-9], dynamic characteristics of a rotor [10], on the dynamic performance of bearing system [11] and of spindles [12]. In [11] the maximum compliance of the spindle tool tip was found to occur at the bending vibrations of a spindle shaft and vary with the preload amount of a spindle bearing.

The preload has a significant effect on the axial stiffness of the machine tool spindle, as shown in [13-14], where the axial stiffness softening and hardening

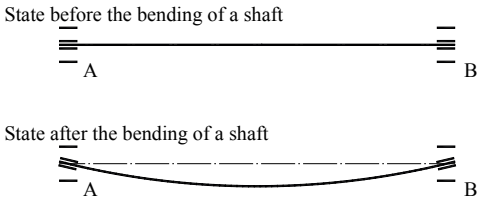

Figure 1 *Tilting of the rings in the bearings due to angular deflection of the shaft [16-17]*

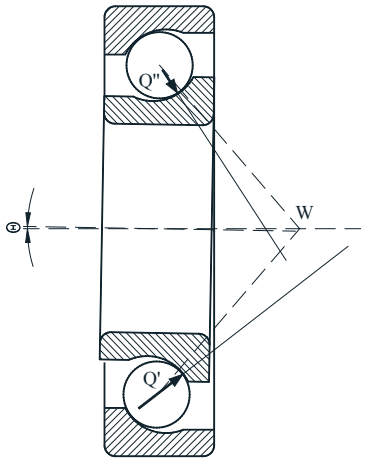

Figure 2 *Direction of internal forces acting in a bearing due to tilting of rings in the bearing by an angle θ: Q' - internal force of the lower ball, Q" - internal force of the upper ball, W - nodal point*

Figure 3 *The emergence of reactionary bending moments in bearings*

characteristics of machine tool spindle are studied. "The results show that when bearing preload reaches a certain relatively large threshold, a "sag" shape occurs in the axial stiffness curve, indicating the "stiffness hardening" characteristic of the spindle. On the other hand, for a small preload no "sag" shape occurs in spindle stiffness curve, indicating the "stiffness softening" characteristic of the spindle. This phenomenon is of great significance for the acquisition of the excellent spindle stiffness properties." [13].

Wear between the rolling elements and raceways has a significant effect on the dynamic characteristics of the bearing, which is the main cause of a bearing failure. The proposed computational models have been developed to investigate the dynamic characteristics of the bearing [15]. However, bearing wear has rarely been studied due to the complexity of the contact load and wear mechanism.

Currently used solutions to the problem define the bearing reaction forces and moments in bearings, assuming that the shaft is perfectly stiff.

However, the susceptibility of the bearings is overlooked. Bearings are considered to be perfectly rigid articulated supports when the reality is different: in most types of bearings, the rings in the bearing tilt relative to each other (Figure 1), which results in contact deformation in the bearing.

Figure 2 shows the tilt of the ring in the bearing. This tilting causes contact deformation where the rolling element is in contact with the raceways, leading to additional internal forces in the bearing. Development of those additional forces in the bearing causes an increase in the pressure Q forces of the rolling elements on the raceways and a change in the action of these forces.

Due to the bearing rings being tilted by an angle θ (Figure 2), the lines of action of the internal force vectors Q 'and Q" pass the nodal point Won the right and as a result create moments of the same signs.

In addition, the lines of action of the forces from all the rolling elements are deflected and this deflection occurs to varying degrees depending on the position of the rolling element on the bearing circumference, resulting in a resultant bending moment in the axial plane of the bearing and shaft. This moment emerges

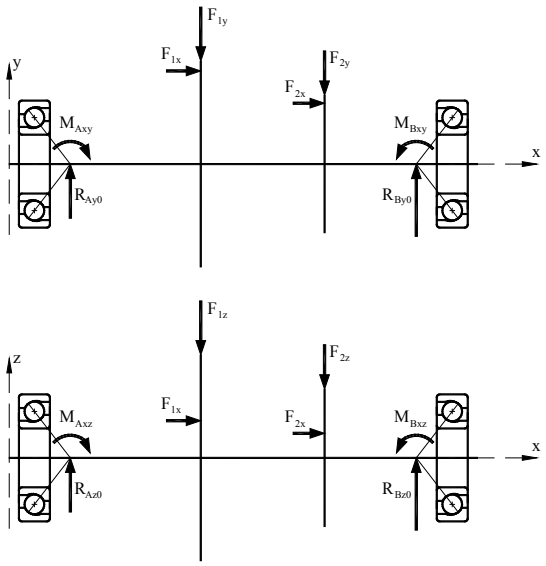

Figure 4 *Calculation of transverse reactions of bearings*

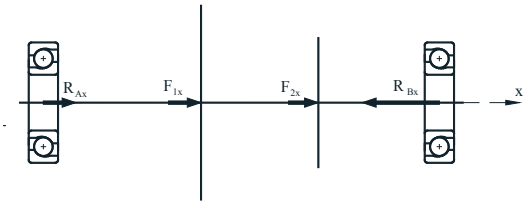

Figure 5 *Calculation of axial reactions of bearings*

simultaneously with the increase of Q forces in relation to the state with no deflection. These bending moments are the bearing's reaction to angular deflection of the shaft and occur in both bearings (Figure 3).

The occurrence of these bending reaction moments in the bearings results in the fact that the bearings are actually loaded completely differently from the simple model based on external forces and support's reactions. Moreover, the resulting reaction bending moments additionally load the shaft and change its deflection line and this affects the bending moment distribution and changes in the reaction of the supports.

In fact, the following loads are exerted on the shaft: (Figure 4 and Figure 5):

- external loads in the form of external forces and moments,
- loads of supports in the form of reaction forces and reaction moments of supports.

All the aforementioned loads have been included in the static equations.

As proven, the values of reaction bending moments are dependent on the shaft deflection line, which means that they are dependent on its stiffness.

If the shaft is loaded in different planes, the shaft deflection line is a three-dimensional line, the shape of which is relatively complicated. Determining the shaft deflection parameters with the use of commonly used formulas is not practical in the case under consideration.

In practice, two methods are used for such complex cases. In the case of many simple shaft loads, the superposition principle can be used, which consists in putting together of the deflection coming from individual forces. Another method used for the complex shaft loads and applied in manuscript, is Mohr's method, based on differential equations describing the geometric parameters of deformations and relationships between loads.

The reaction moments generated in the bearings are the bearings reaction to shaft angular deflection. The values of the reaction bending moments depend on the shaft deflection line and therefore they depend on its stiffness.

When calculating the bearing service life, in addition to shaft elasticity, bearing radial, axial and bending elasticity must be taken into account. The radial and axial elasticity is determined by the dependence of the radial and axial force acting on the bearing and the radial and axial displacement of the rings in the bearings.

On the other hand, bending elasticity is expressed by the dependence of the bending moment, developed in the bearing, on the angular deflection of the rings in the bearing.

Not only the radial and axial reaction, but the reaction moment of each bearing is considered in the static equations of the system, as well. It is worth noting that there is a feedback: the radial displacements in the bearings correspond to the deflections of the shaft on the

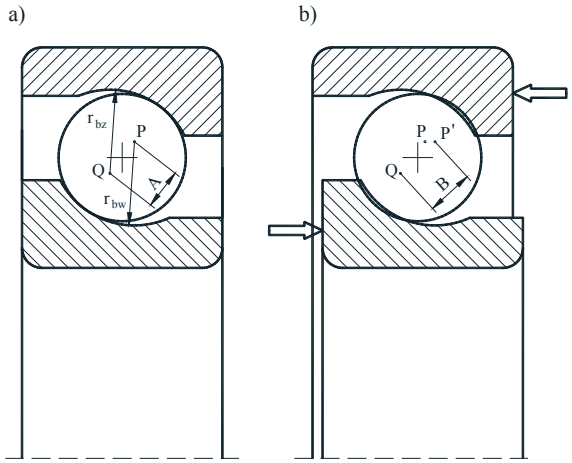

Figure 6 *Ring displacement due to loading and preload*

supports and the angular deflections of the bearing rings are determined by the deflection line of the shaft and this deflection line is affected by the reaction moments of the bearings, which affect the angular deflections of the rings.

The bearing reactions result from the internal forces acting between the bearing elements, which in turn depend on the mutual displacements of the bearing elements.

The pressure force between the rolling part (ball) and the raceway of the ring of the ball bearing is the cause of the contact deformation. This deformation is spatial, i.e. three-dimensional. The area of the deformed surface can be considered elliptical and the profile - parabolic. There is a close correlation between the force Q and the dimensions of the contact ellipse and the depth of deformation in both contacting elements.

Figure 6 shows a half section of the bearing. Figure 6a shows the unloaded condition. In this condition, the ball adheres to both rings without distortion. The center of curvature of the inner ring raceway is at point P and the outer ring is at point Q. The spacing between them is A.

Figure 6b shows the condition after the axial loading of the bearing (obviously greatly exaggerated) and due to the application of preload. The inner ring has been shifted relative to the outer ring and the center of its raceway curvature has moved to the point P '. The circle symbolizing the ball now penetrates a certain depth into the profiles of both rings, which causes contact deformation. The contact strains can be determined from the formula:

$$\delta = B - A = P'Q - PQ\,. \tag{1}$$

This principle determines the normal contact deformation for an arbitrarily positioned ball due to a displacements of the inner ring relative to the outer ring. Before presenting this spatial analysis, it is necessary to define the geometrical design features of the bearing.

The calculation of deformations in the contact between any sphere and rings can be done using the vector calculus. It will be more correct to explain this procedure in a three-dimensional drawing showing all the displacements. The method shown is used in this procedure and is illustrated in Figure 7. The starting point is an approximation of the rings in the bearing (inner relative to outer) on which this ball is located. The measure of this approximation is the local distance between the circles OK_p and OK_q. This can be delineated by considering the change in position of point P to position P'. This transition consists in the displacement of the inner ring in the x, y, z directions and its deflection about around the y and z axes:

- shift in the x direction: f_x
- shift in the y direction: f_y
- shift in the z direction: f_z
- tilt with respect to y axis: $r_p \cdot \Theta_y \cdot \sin \psi$
- tilt with respect to z axis: $r_p \cdot \Theta_z \cdot \cos \psi$.

The point P' has a different axial plane from the point P because it experiences some circumferential shift. This new plane is indicated in Figure 7 by the vertices of ae triangle BP'Q'. Therefore, the distance between the circles OK_p and OK_q, is the distance between the points P' and Q' to be measured. For a more accessible illustration of the components of the displacement of point P to P', an additional Figure 8 is provided, showing the plane BP'Q', where point P is converted to point PP. The displacements f_y and f_z are projected onto the plane BP'Q'. The difference between the distances P'Q' and PP Q' defines the value of the ring approximation.

After determining the rapprochement of the rings δ and the Hertzian parameters of the contact δ* and Σρ, it is now possible to determine the force Q at the contact point under consideration.

Knowing the Q forces acting between the balls and rings allowed to determine the reaction forces and the reaction moments for the spatial force system. The notation of the reactions is shown in Figure 9.

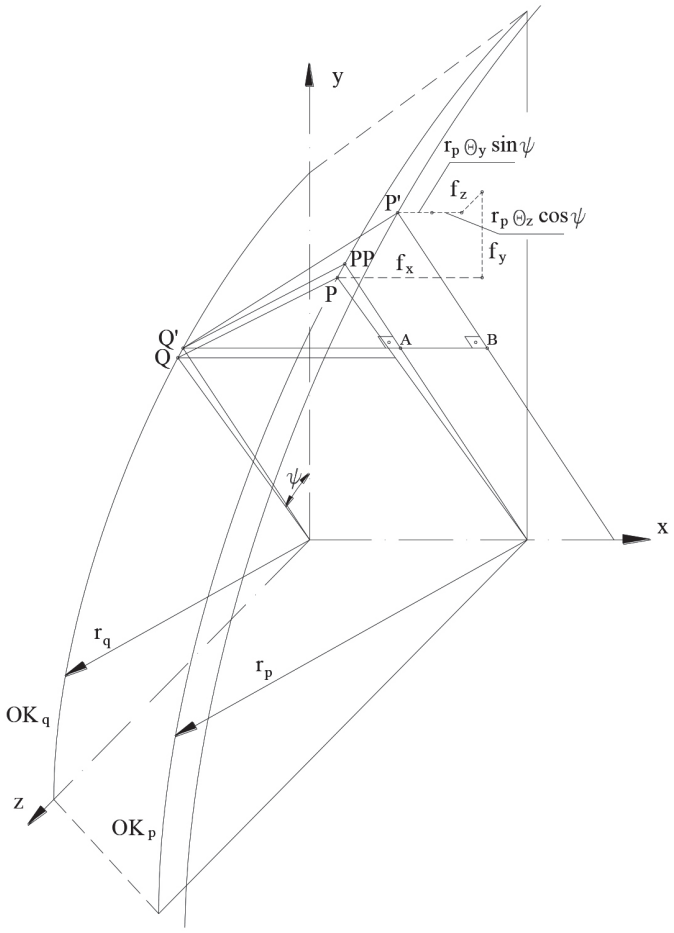

Figure 7 *Local approximation of rings*

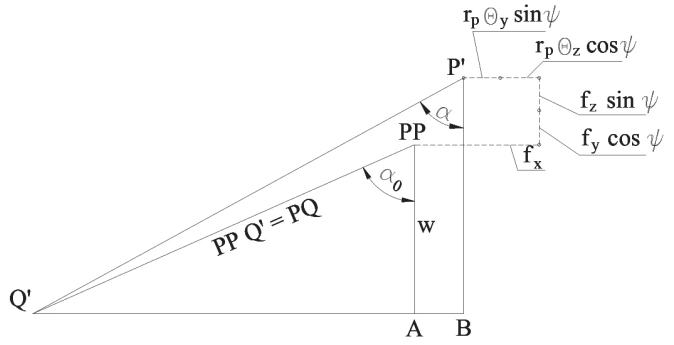

Figure 8 *Illustration in the BP 'Q' plane of the principle of calculating the local rapprochement of the rings*

The upper figure in the perspective view shows the arc of the centers of curvature of the outer ring raceway. The Q forces are applied to the points on this arc, which act between the rolling elements and the bearing raceway. They are deviated from the y-z plane by the angle α. As a result of the projection of the Q forces on the assumed axes of symmetry, one obtains the following formulas:

$$Q_x = Q \cdot \sin\alpha\,, \tag{2}$$

$$Q_r = Q \cdot \cos\alpha\,, \tag{3}$$

$$Q_y = Q_r \cdot \cos\psi = Q \cdot \cos\alpha \cdot \cos\psi\,, \tag{4}$$

$$Q_z = Q_r \cdot \sin\psi = Q \cdot \cos\alpha \cdot \sin\psi\,, \tag{5}$$

$$M_{xz} = Q \cdot \frac{r_q \cdot (r_{bw} + r_{bz} - D_k)}{w} \cdot \sin(\alpha - \alpha_0) \cdot \sin\psi\,, \tag{6}$$

$$M_{xy} = Q \cdot \frac{r_q \cdot (r_{bw} + r_{bz} - D_k)}{w} \cdot \sin(\alpha - \alpha_0) \cdot \cos\psi\,. \tag{7}$$

Equations (2) ÷ (7) define the loads occurring on one, arbitrary, rolling element.

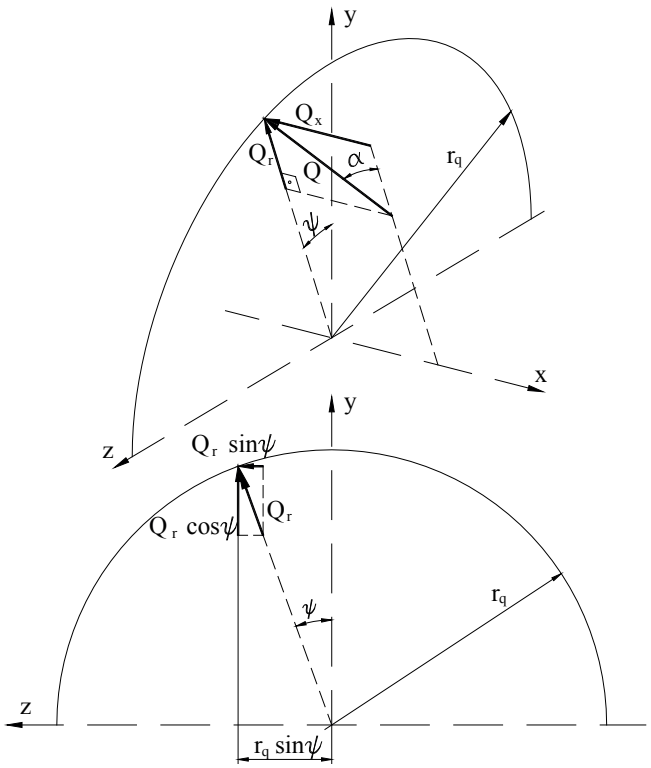

Figure 9 *Determining the reaction of bearing*

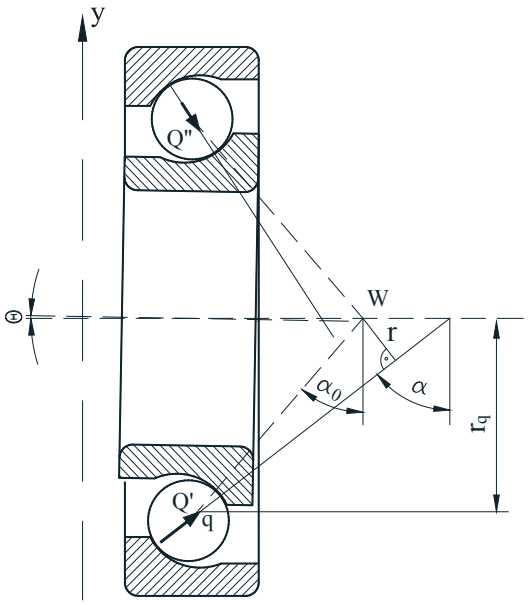

Figure 10 *Determining the reaction moment of a bearing [18-19]*

The moment from the force Q is to be determined with respect to the point W, which is measured at the point of support of the shaft on the bearing. This calculation is shown in Figure 10. The force Q is applied at the center of the outer ring raceway curve, denoted as q. The moment of force Q coming out of any sphere (here a sphere lying in the plane of the diagram is chosen) is:

$$M = Q \cdot r\,. \tag{8}$$

The total bearing reactions and reaction moments are the result of the interaction of each rolling element in the bearing and are determined by adding the forces and moments resulting from rolling elements under the normal deformation:

$$R_x = \sum (Q \cdot \sin\alpha)\,, \tag{9}$$

$$R_r = \sum (Q \cdot \cos\alpha)\,, \tag{10}$$

$$R_y = \sum (Q \cdot \cos\alpha \cdot \cos\psi), \tag{11}$$

$$R_z = \sum (Q \cdot \cos\alpha \cdot \sin\psi), \tag{12}$$

$$M_{xz} = \sum \left[Q \cdot \frac{r_q \cdot (r_{bw} + r_{bz} - D_k)}{w} \cdot \sin(\alpha - \alpha_0) \cdot \sin\psi \right], \tag{13}$$

$$M_{xy} = \sum \left[Q \cdot \frac{r_q \cdot (r_{bw} + r_{bz} - D_k)}{w} \cdot \sin(\alpha - \alpha_0) \cdot \cos\psi \right]. \tag{14}$$

The formulas presented here allowed the reactions of the two shaft bearings to be determined separately, based on their separate internal deformations.

The above shows determination of the shaft support reactions based on the shaft loads and determination of the bearing reactions as a response to the deformations taking place in them. The shaft supports are, of course, the bearings. Both reactions must therefore be respectively equal to each other. It is one of the components of the bearing balance. The first is the equilibrium of the reaction in the directions perpendicular to the shaft axis, i.e. y and z. If the lateral reaction, calculated as the support reaction, was greater than the bearing reaction resulting from internal deformations in it, for example:

$$R_{Ay0} > R_{Ay}, \tag{15}$$

$$\text{or } R_{Az0} > R_{Az}, \tag{16}$$

$$\text{or } R_{By0} > R_{By}, \tag{17}$$

$$\text{or } R_{Bz0} > R_{Bz}, \tag{18}$$

then the calculation procedure increases the internal displacement in the corresponding bearing (A or B) in the appropriate direction (x or y), so as to satisfy all the above equations. In the event of the opposite sign of inequality, the corresponding displacement in the corresponding bearing is reduced.

In the direction of the shaft axis, the balance of the axial external forces and the axial reactions of the bearings is checked. The resultant of these forces:

$$W_x = R_{Ax} + \sum F_{ix} - R_{Bx}, \tag{19}$$

should be zero. If it is less than zero, the calculation procedure shifts the shaft along with the inner rings of the bearings to the left in order to increase the left bearing deformation and consequently increase the R_{Ax} force and at the same time reduce the R_{Bx}. If, on the other hand, this resultant $W_x > 0$, then the calculation procedure shifts the shaft along with the inner rings of the bearings to the right in order to reduce the R_{Ax} force and at the same time increase the R_{Bx}.

The iterative process presented above, used in the computer program, makes it possible to calculate such displacements and tilts of the inner rings in relation to the outer rings in both bearings, that all the equilibrium equations are simultaneously satisfied.

The absolute equivalent load on the ring, moving in relation to the load, is equivalent to the time-averaged load of the ball circling the bearing Q_{sr}. This value is calculated in the computer program according to the known dependence taking into account the equivalent effort of the material subjected to variable loads:

$$Q_{sr} = \frac{1}{Z} \sum_{i=1}^{Z} Q_i^3. \tag{20}$$

The equivalent load of a point contact radial bearing is calculated from the formula:

$$P = \frac{0.2288}{0.5625} \cdot Z \cdot Q_{sr} = 0.4068 \cdot Z \cdot Q_{sr}. \tag{21}$$

The angular contact ball bearing belongs to the deep groove bearings with point contact. The fatigue strength of the raceways and balls of an angular contact bearing depends in the same way on their averaged load as in a deep groove ball bearing, provided that the total load is taken into account, not only its radial component. In the developed procedure, the total loads are calculated. Therefore, the formula was adopted for the angular contact ball bearing.

Based on the Weibull theory, an expression was obtained:

$$L = \left(\frac{C}{P} \right)^p. \tag{22}$$

The number L is the number of million revolutions the bearing can make before the raceway or rolling elements are damaged. The exponent of the power p is a number with different values depending on the bearing type. For the ball bearings, p = 3.

2 The calculation method used

In order to solve the problem, it was necessary to combine such issues as: deflection line of machine shaft for the complex external load, dislocations of inner rings in relation to the outer ones as a result of loads and of preload, elastic contact deformations in the points of contact of rolling parts with the track in both bearings of the system, calculations of contact forces in bearings, based on contact deformations, balance between inner (contact) forces and outer loading of the whole bearing, calculations of durability of bearings based on these contact forces.

The adoption of a correct computational model is a crucial step towards finding a theoretical solution to the problem. On the correctness of the model depends the scope of the considered phenomena, the degree

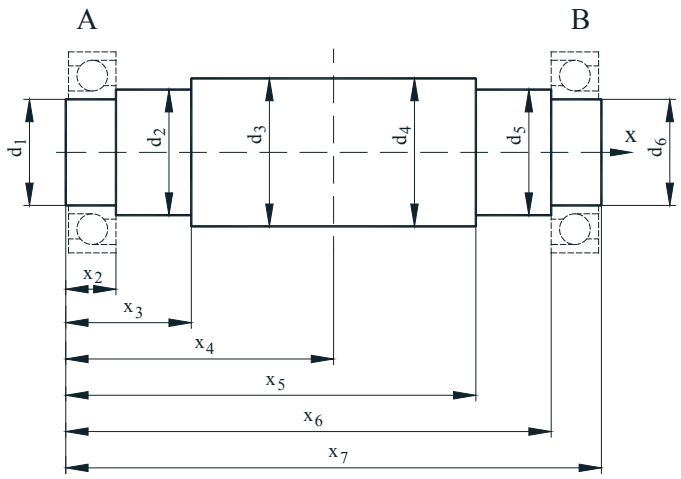

Figure 11 *Sketch of a model shaft*

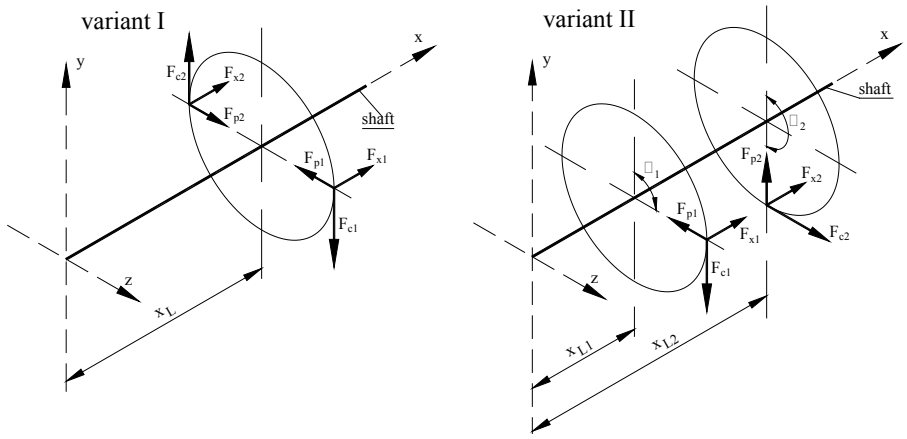

Figure 12 *Load variants adopted*

of approximation to reality and the amount of work needed to apply the solution. For the present study, used a method developed by the author, which was applied in papers [20-24] and others.

3 Analytical considerations

These types of bearings work in arrangements and must be considered in arrangements. Forces that occur in bearings depend, among others, on the load bearing, shaft deflection. The bearing load or the shaft deflection line depends again on the way the external shaft is loaded. Possibilities are endless, therefore a specific construction had to be assumed by the author.

The assumed construction was a model shaft (Figure 11) with two 7212B angular ball bearings of a dynamic capacity of C=57200 N, according to [25].

The model shaft has the following dimensions: x_2 = 22 mm, x_3 = 100 mm, x_4 = 200 mm, x_5 = 300 mm, x_6 = 371 mm, x_7 = 400 mm, d_1 = 60 mm, d_2 = 67 mm, d_3 = 75 mm, d_4 = 75 mm, d_5 = 67 mm, d_6 = 60 mm. The bearing was a subject to calculations for loadings different in values and differently placed. Variants of locations are shown in Figure 12. In one variant of location (variant I) it is assumed the load is assumed to be on either side of a single gear located at a distance x_L distance from the end of the shaft. In another variant (variant II) loads are applied on two gears placed at x_{L1} and x_{L2} distances from the end of the shaft. Location of points of application is defined by angles β_1 and β_2.

The locations of the load planes were taken in relation to the shaft length L_w, which corresponds to dimension x_7:

For variant I of the location (Figure 12 - left): $x_L = 0.3\ L_w$, $x_L = 0.4\ L_w$, $x_L = 0.5\ L_w$, $x_L = 0.6\ L_w$ or $x_L = 0.7\ L_w$.

For variant II of the location (Figure 12 - right): $x_{L1} = 0.4\ L_w$, $x_{L2} = 0.6\ L_w$, for the angles: $\beta_1 = \beta_2 = 90^o$ and $\beta_1 = 90^o$, $\beta_2 = 180^o$ or $\beta_1 = 90^o$, $\beta_2 = 270^o$.

Diameter of the rolling: D_t = 200 mm.

It has been assumed, that loads in both the points presented in Figure 12 are identical. ($F_{c1} = F_{c2}$, $F_{p1} = F_{p2}$, $F_{x1} = F_{x2}$). The diameters of the gears are the same.

The circumferential load F_{c1} on the alleged gear F_{c1} depends on dynamic capacity of the bearing and will be assumed as 0.1 C, when F_{p1}=0.36 F_{c1}.

Characteristics of durability of bearings, when considering the preload for the obtained values, are presented in the Figures 13÷19:

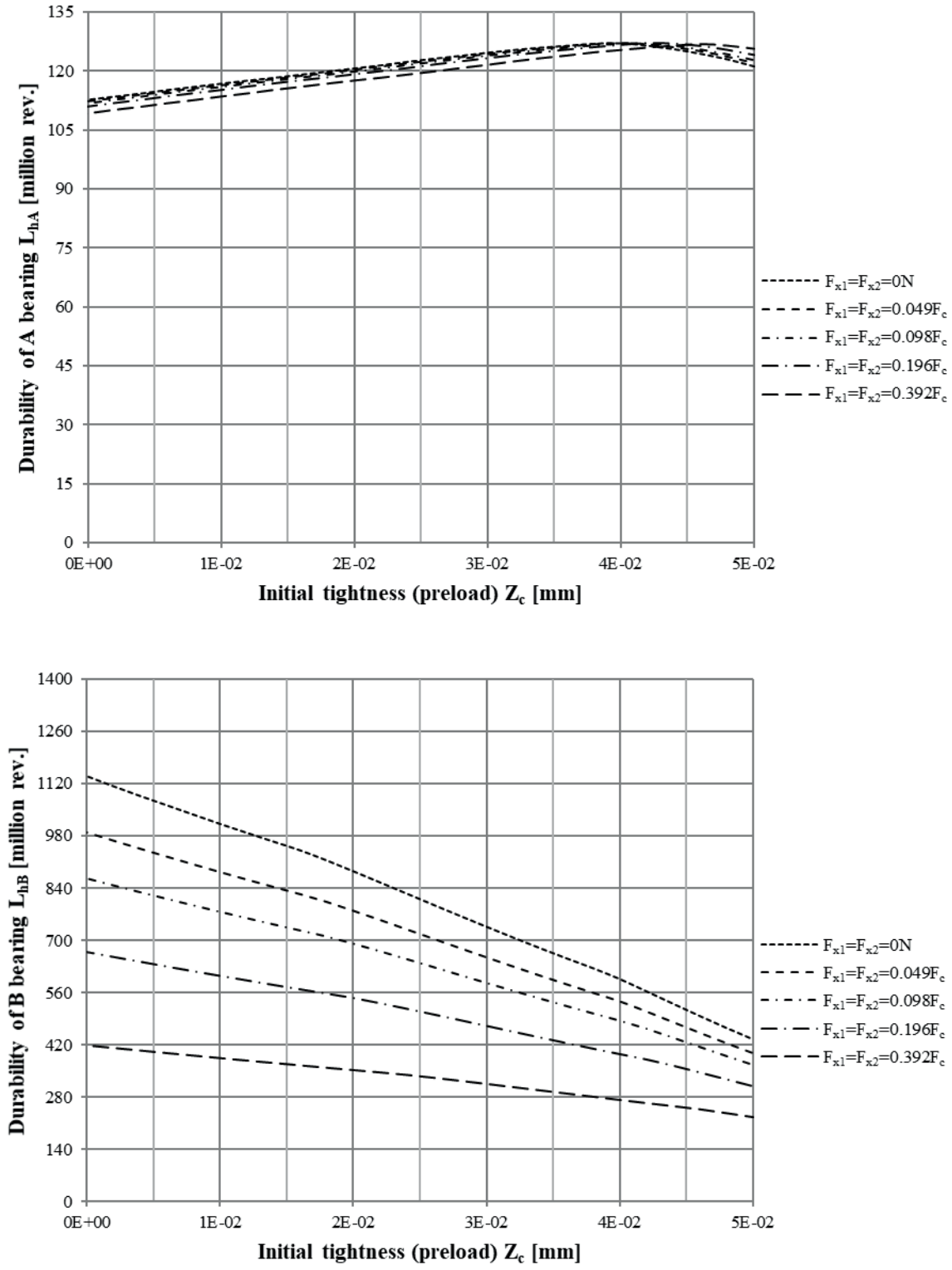

Figure 13 *Durability of bearings A and B for the load plane x_L = 0.3 L_W for variant I of the load*

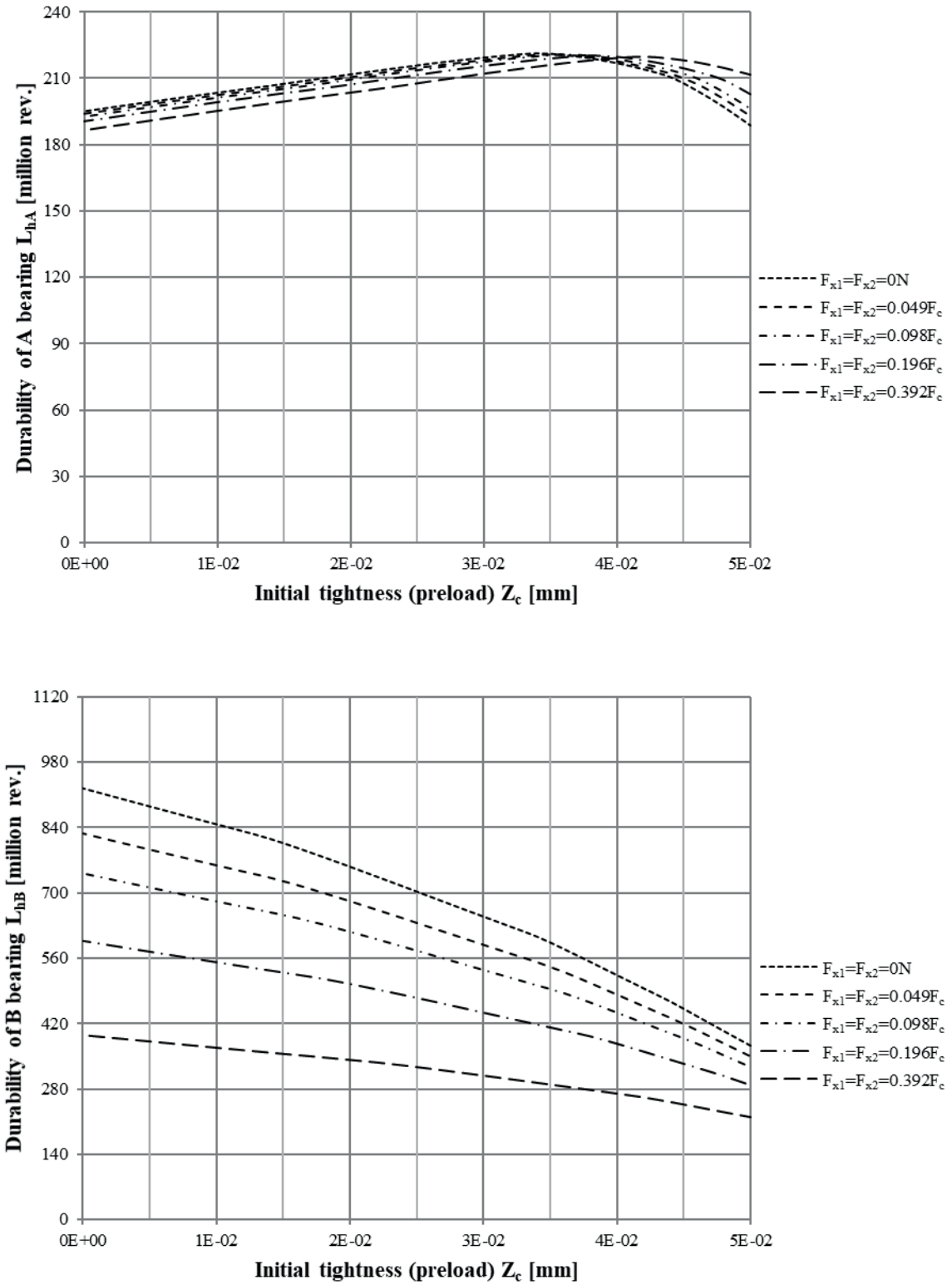

Figure 14 *Durability of bearings A and B for the load plane x_L = 0.4 L_W for variant I of the load*

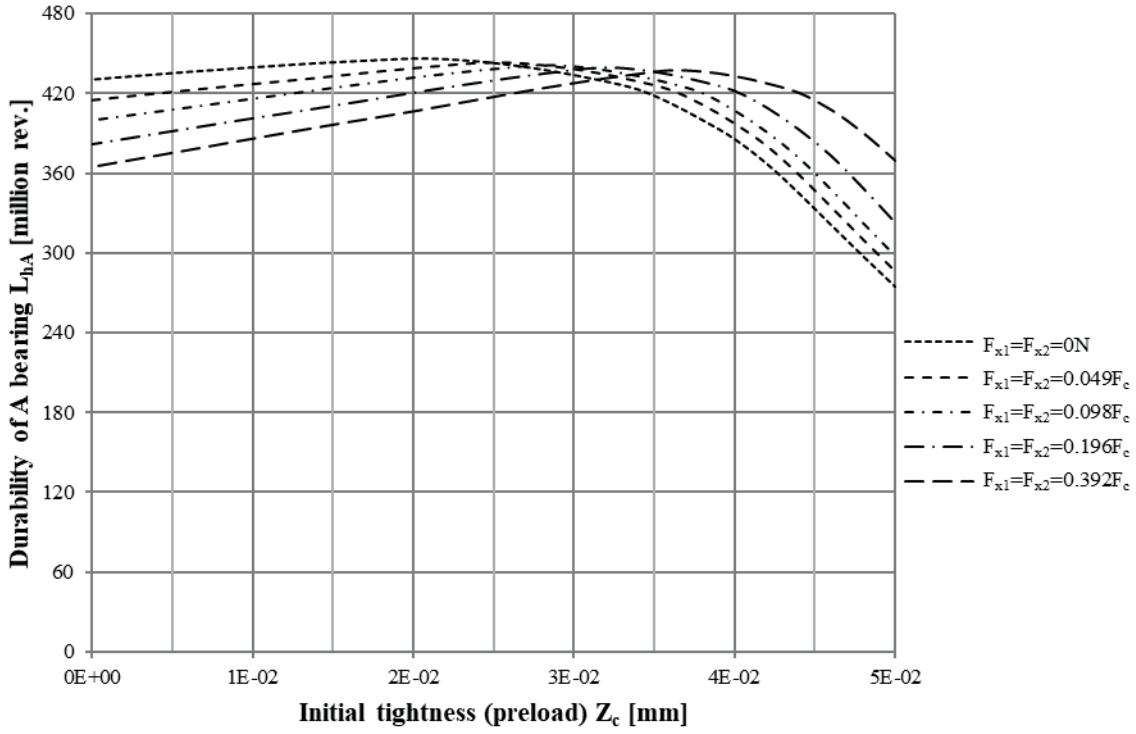

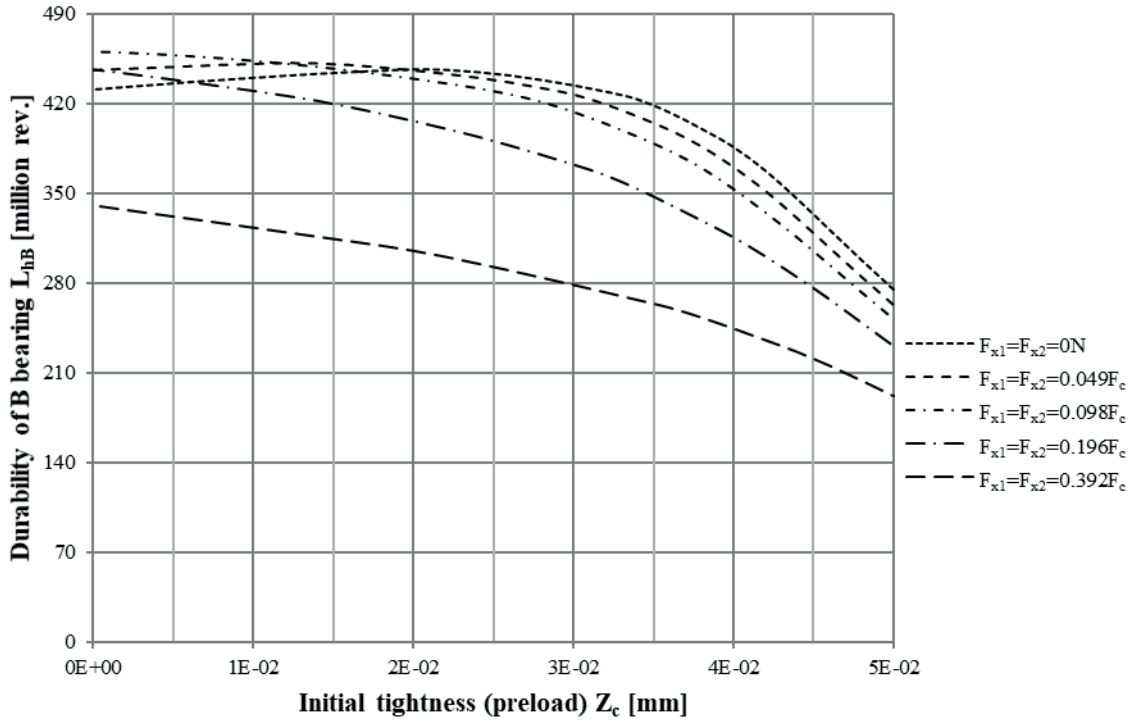

Figure 15 *Durability of bearings A and B for the load plane x_L =0.5 L_W for variant I of the load*

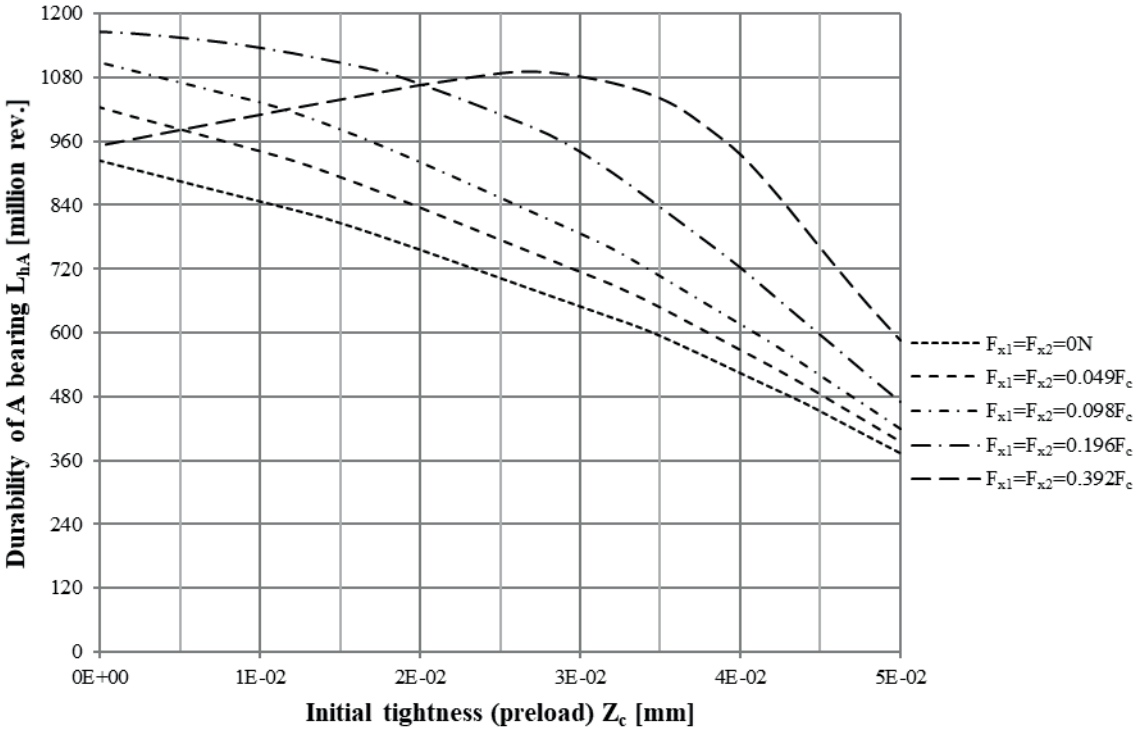

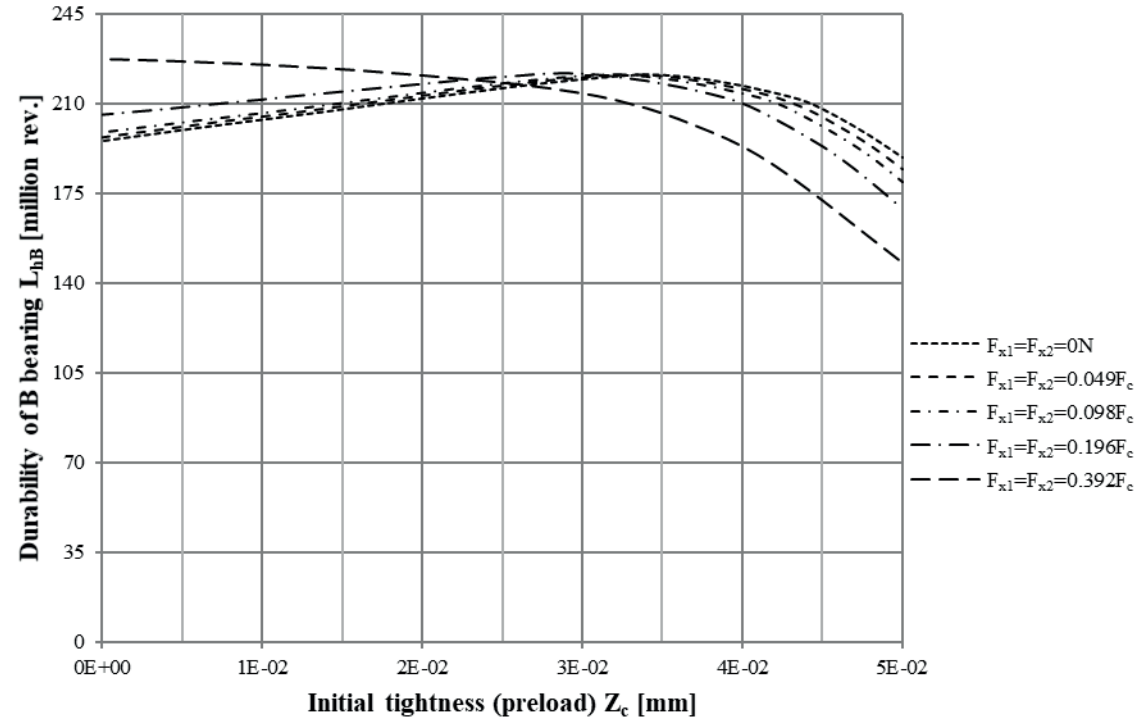

Figure 16 *Durability of bearings A and B for the load plane $x_L = 0.6\ L_W$ for variant I of the load*

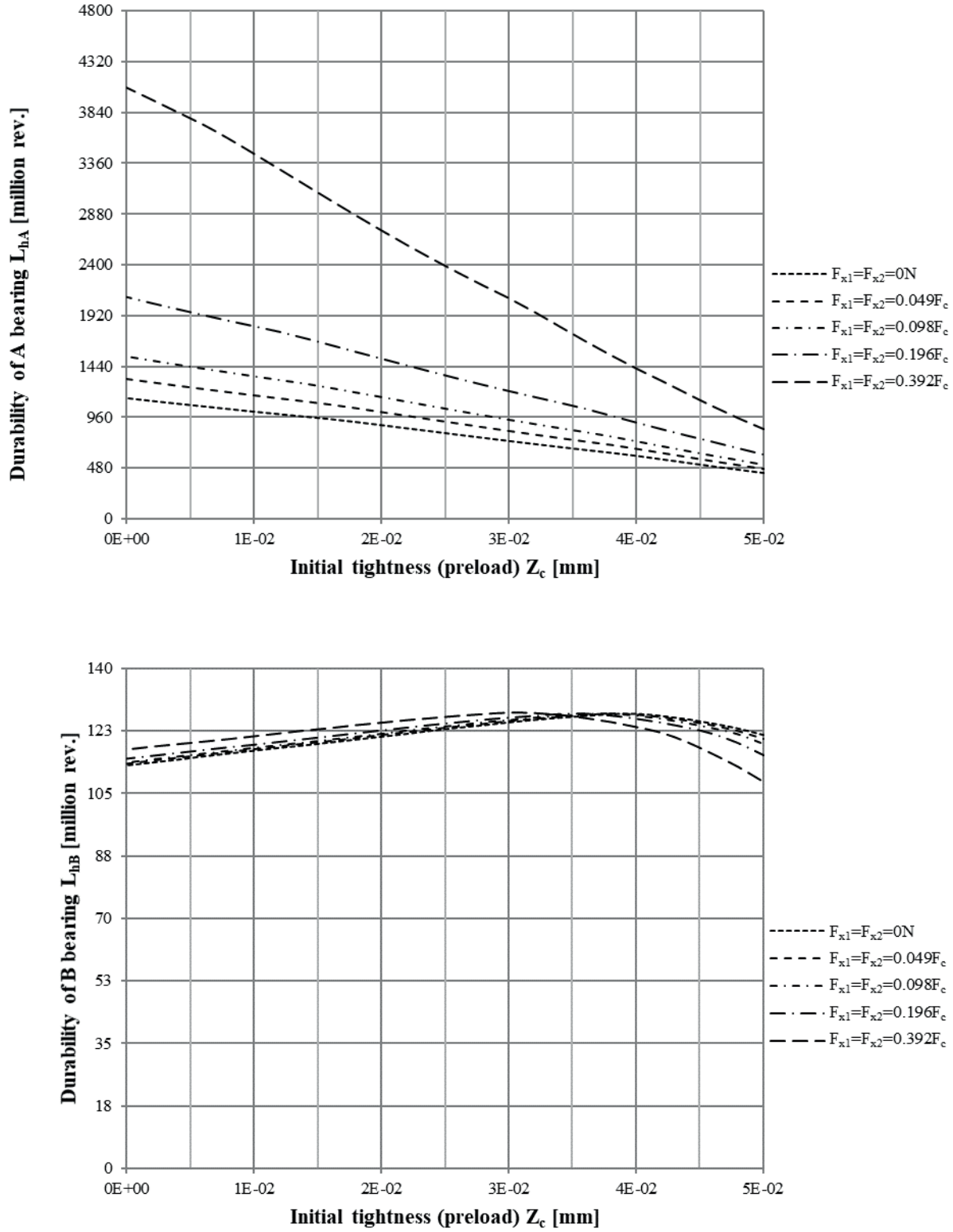

Figure 17 *Durability of bearings A and B for the load plane $x_L = 0.7\ L_W$ for variant I of the load*

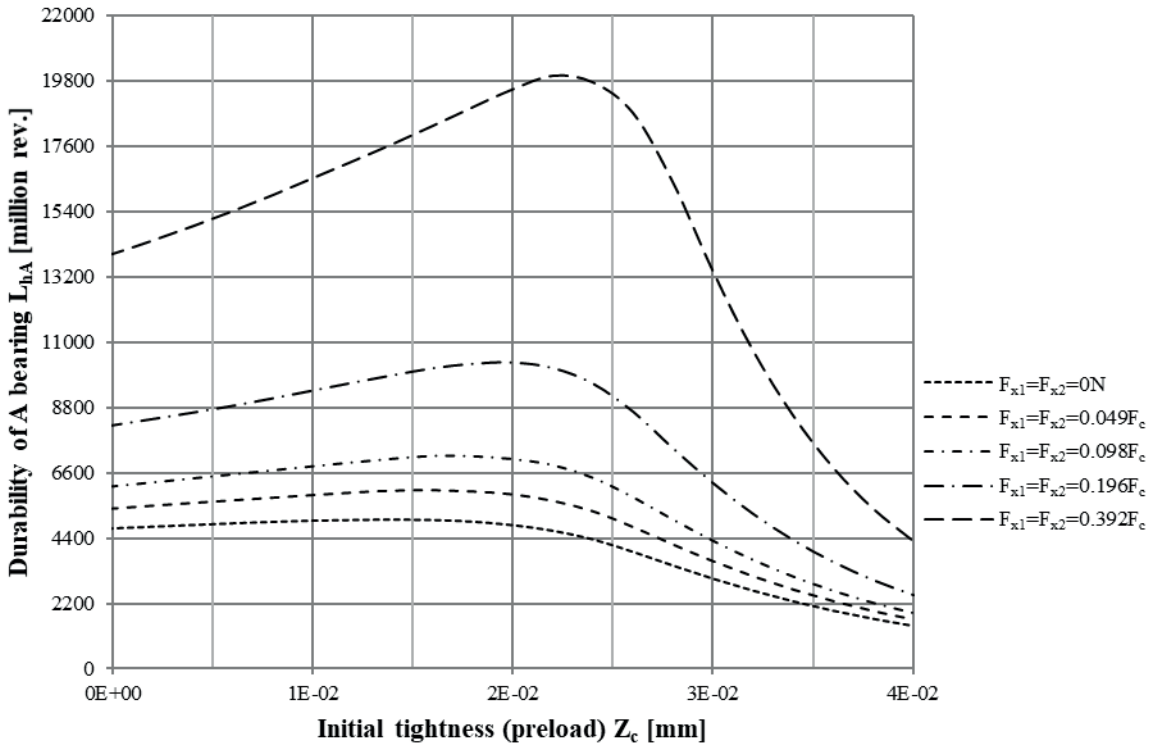

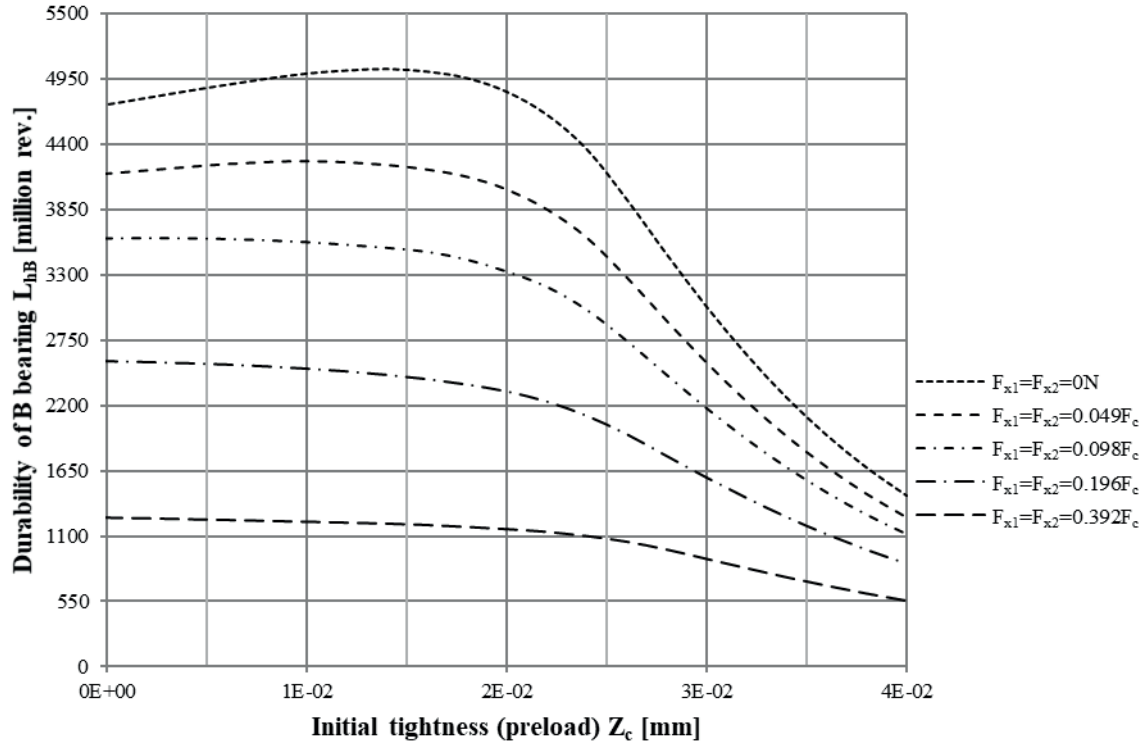

Figure 18 *Durability of bearings A and B for variant II of the loading and for the angles of the load applications $\beta_1 = 90^o$, $\beta_2 = 90^o$*

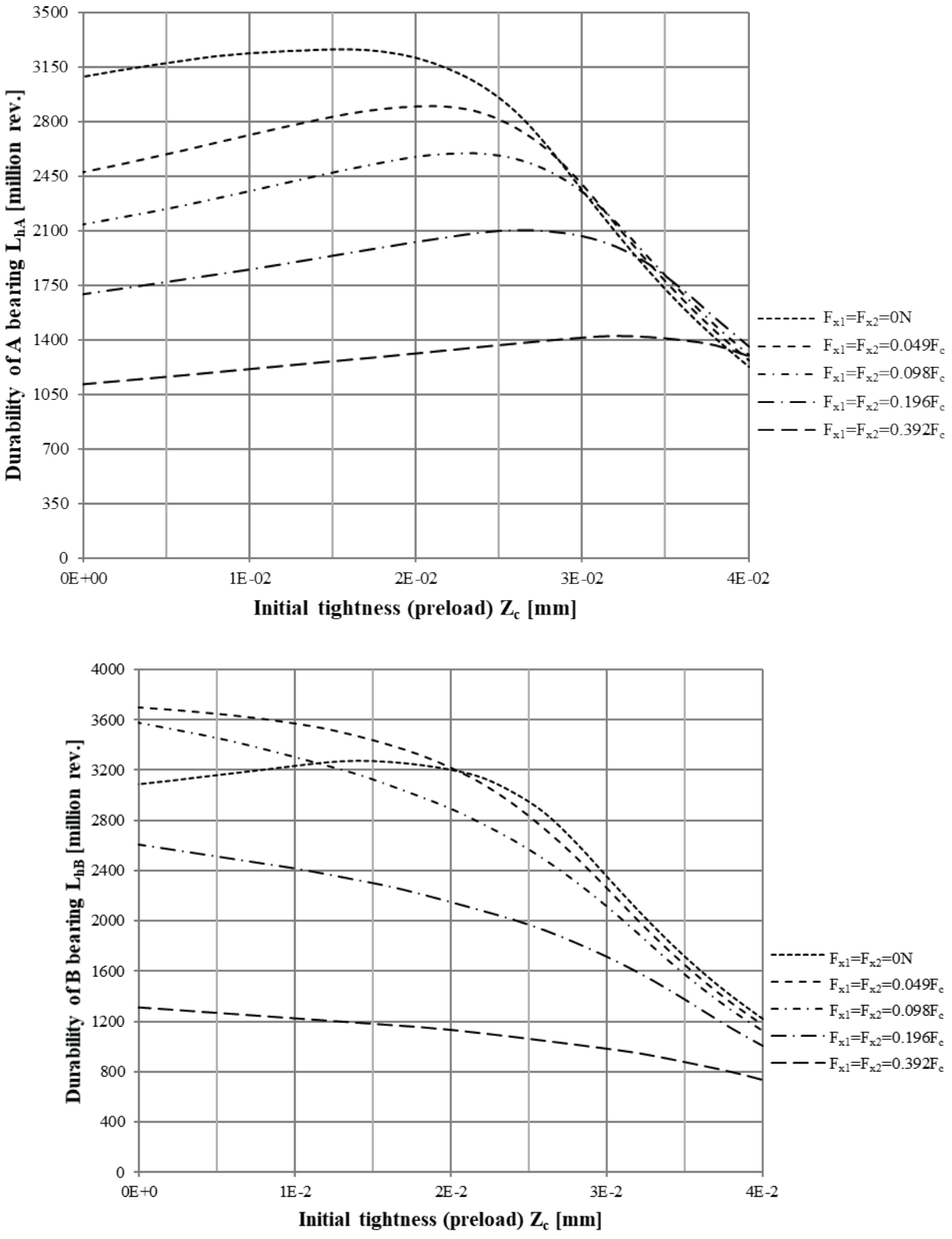

Figure 19 *Durability of bearings A and B for variant II of the loading and for the angles of the load applications $\beta_1 = 90^o$, $\beta_2 = 180^o$*

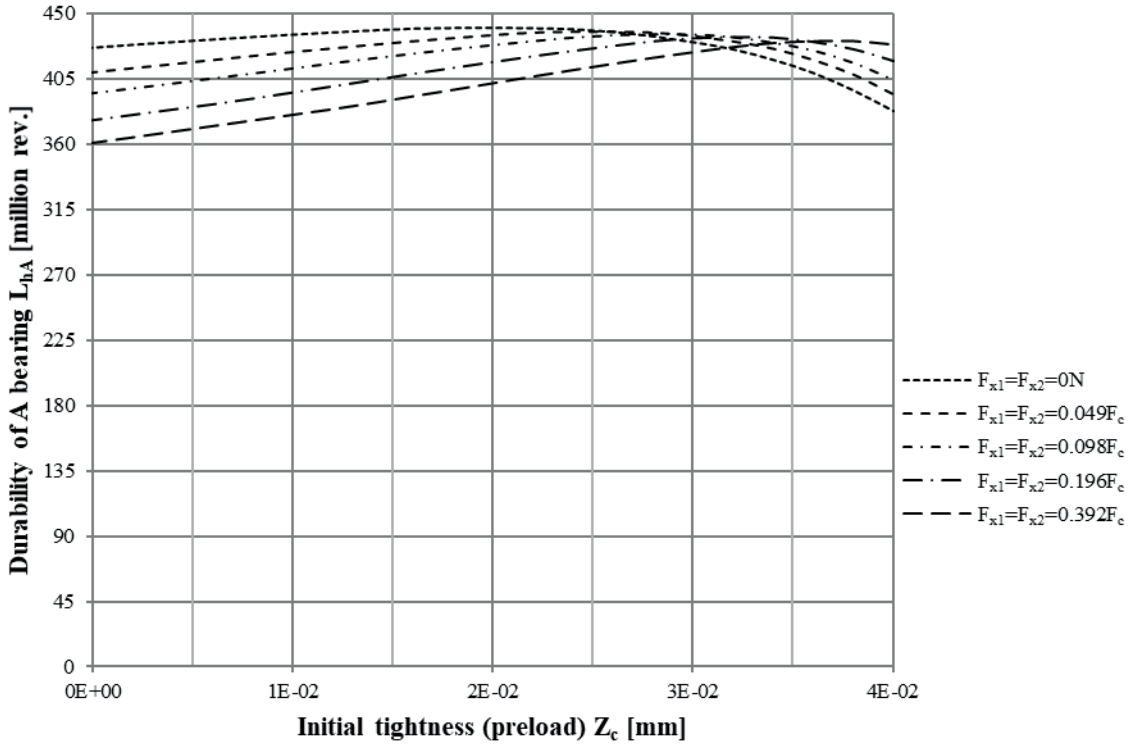

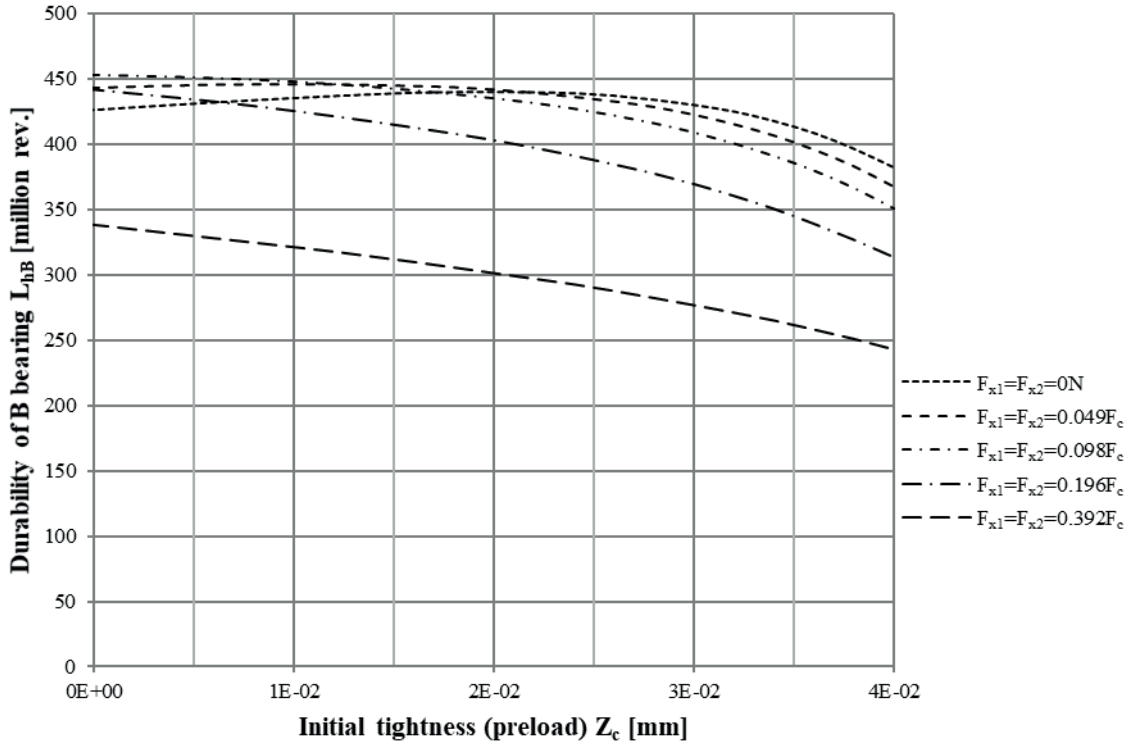

Figure 20 *Durability of bearings A and B for variant II of the loading and for the angles of the load applications $\beta_1 = 90^o$, $\beta_2 = 270^o$*

4 Deduction

The following observations have been made based on Figures 13÷20:

When loads are applied to the shaft located closer to the left bearing, then, independently of the value of the cross-bending and axial loads, together with the increase of preload $Z_{c,}$ durability of bearing A increases slowly up to a certain value Z_c and then falls rapidly. The maximum value is reached for different Z_c values, depending on the values of loadings. In contrast, the life of the right bearing (B) under these conditions decreases markedly over the entire range of increasing preload. Furthermore, the life curves of bearing B have different levels depending on the axial force, which is understandable since it is directed at the right bearing.

When the forces are applied exactly in the middle between the bearings, the life curve A bearing is similar to the previous case, which means they obtain maximum values. However, in this case these maximum values are visibly "dislocated" in correlation to one another, depending on the axial load values. In contrast to the previous load placement, in this case certain curves of durability of the bearing B (the right one) also obtain maximum values. Those are the curves that correspond to the lowest values of axial force (below 0.1 F_c). For the higher values of axial force, the characteristics of durability of the bearing B have a falling course.

If the loads are applied closer to the bearing on the right side, both the bearing life of bearing A and B vary with the axial force. For a large value of the axial force (above 0.2 Fc), the life curves of bearing A increase to a certain maximum value, but for a smaller axial force these curves decrease monotonically as the preload value increases from 0. On the other hand, the life curves of bearing B behave in the opposite way: the appearance of maximum values can be observed when the axial force is less than 0.2 Fc. When the axial force is higher, the life characteristics of bearing B decrease, but not so sharply.

With the loads applied to the two different wheels, located as in Figure 12, the character of the curves resembles the course characteristic of the position of the load plane exactly in the center of the shaft. All the curves durability of the bearing A demonstrate maxima located in a similar range of preload as in the case of central location of one plane of the load. Whereas out of the durability curves of the bearing B, only the one corresponding to the axial force 0 reaches maximum for the positive value of preload. Other curves are decreasing.

Advantageous durability characteristics for bearings are visible in all the graphs. A small number of lines fall moderately with the increase of preload. However, most of the lines have a rising course, at times, even a significantly rising one.

5 Conclusion

Observations presented above prove, that only when the plane of loading is placed at a half the distance between the bearings and with a low axial load (below 0.1 F_c), a preload enables achieving the increase in durability of both bearings. In all the other cases, the life characteristics of A and B bearings are opposite: when one characteristics increases, the other characteristics simultaneously decreases.

However, it would be too superficial to assume that the use of preload in bearings is usually a harmful factor. It is known that as a result of preload an increase of longitudinal stiffness of a bearing system is obtained, which is beneficial. The observed phenomena mean only that characteristics of durability, when observed separately, will not provide an answer to the question about the optimum value of preload for a specific shaft load.

An application of variable preload is necessary because it has a big impact on bearings' performance, which is shown in [26].

In article [27] a new automatic variable preload system has been proposed. This system fits the preload, however it only depends on the spindle rotational speed. It is crucial to remember that the internal contact feature and thermally induced dynamic preload are essential for a ball bearing which is one of the key problems associated with thermal instability and lock-up problems at high rotational speed.

In [28] is presented a thermo-mechanical coupling model for the angular contact ball bearing with preload and temperature compensation, for the purpose of dynamic preload monitoring.

An interesting solution of the preload has been shown in [29] where the piezoelectric actuators have been used. Furthermore, this article may form the basis for future research into intelligent preload control technology, as well as investigating the thermal-mechanical-dynamic characteristics of the high-speed bearing system.

References

[1] AQUIRREBEITIA, J., PLAZA, J., ABASOLO, M., VALLEJO, J. Effect of the preload in the general static load-carrying capacity of four-contact-point slewing bearings for wind turbine generators: theoretical model and finite element calculations. *Wind Energy* [online]. 2014, **17**(10), p. 1605-1621. eISSN 1099-1824. Available from: https://doi.org/10.1002/we.1656

[2] CHOI, CH.-H., LEE, CH.-M. A variable preload device using liquid pressure for machine tools spindles. *International Journal of Precision Engineering and Manufacturing* [online]. 2012, **13**, p. 1009-1012. ISSN 2234-7593, eISSN 2005-4602. Available from: https://doi.org/10.1007/s12541-012-0131-2

[3] BAI, CH., ZHANG, H., XU, Q. Effects of axial preload of ball bearing on the nonlinear dynamic characteristics of a rotor-bearing system. *An International Journal of Nonlinear Dynamics and Chaos in Engineering Systems* [online]. 2008, **53**(3), p. 173-190. ISSN 0924-090X, eISSN 1573-269X. Available from: https://doi.org/10.1007/s11071-007-9306-2

[4] CAO, H., HOLKUP, T., ALTINTAS, Y. A comparative study on the dynamics of high speed spindles with respect to different preload mechanisms. *The International Journal of Advanced Manufacturing Technology* [online]. 2011, **57**(9), p. 871-883. ISSN 0268-3768, eISSN 1433-3015. Available from: https://doi.org/10.1007/s00170-011-3356-9

[5] CHEHG, H., ZHANG, Y., LU, W., YANG, Z. Research on the effect of structural and material parameters on vibrations based on quasi-static model of bearings. *Journal of the Brazilian Society of Mechanical Sciences and Engineering* [online]. 2020, **42**(11), 578. ISSN 1678-5878, eISSN 1806-3691. Available from: https://doi.org/10.1007/s40430-020-02659-x

[6] GAOFENG, H., WEIGUO, G., YE, CH., DAWEI, Z., YANLING, T., XIANGYANG, Q., HONGIJE, Z. An experimental study on the rotational accuracy of variable preload spindle-bearing system. *Advances in Mechanical Engineering* [online]. 2018, **10**(5), p. 1-14. ISSN 1687-8132, eISSN 1687-8140. Available from: https://doi.org/10.1177/1687814018776171

[7] GU, J., ZHANG, Y., LIU, H. Influences of wear on dynamic characteristics of angular contact ball bearings. *Meccanica* [online]. 2019, **54**(7), p. 945-965. ISSN 0025-6455, eISSN 1572-9648. Available from: https://doi.org/10.1007/s11012-019-00996-3

[8] HU, G., ZHANG, D., GAO, W., CHEN, Y., LIU, T., TIAN, Y. Study on variable pressure/position preload spindle-bearing system by using piezoelectric actuators under close-loop control. *International Journal of Machine Tools and Manufacture* [online]. 2017, **125**, p. 68-88. ISSN 0890-6955. Available from: https://doi.org/10.1016/j.ijmachtools.2017.11.004

[9] HUNG, J.-P., LAI, Y.-L., LUO, T.-L., SU, H.-CH. Analysis of the machining stability of a milling machine considering the effect of machine frame structure and spindle bearings: experimental and finite element approaches. *The International Journal of Advanced Manufacturing Technology* [online]. 2013, **68**(9-12), p. 2393-2405. ISSN 0268-3768, eISSN 1433-3015. Available from: https://doi.org/10.1007/s00170-013-4848-6

[10] HWANG, Y.-K., LEE, CH.-M. A review on the preload technology of the rolling bearing for the spindle of machine tools. *International Journal of Precision Engineering and Manufacturing* [online]. 2010, **11**(3), p. 491-498. ISSN 2234-7593, eISSN 2005-4602. Available from: https://doi.org/10.1007/s12541-010-0058-4

[11] SIM, K., LEE, Y.-B., KIM, T. Effects of mechanical preload and bearing clearance on rotor dynamic performance of lobed gas foil bearings for oil-free turbochargers. *Tribology Transactions* [online]. 2013, **56**(2), p. 224-235. ISSN 1040-2004, eISSN 1547-397X. Available from: https://doi.org/10.1080/10402004.2012.737502

[12] HWAN, Y.-K., LEE, CH.-M. Development of a simple determination method of variable preloads for high speed spindles in machine tools. *International Journal of Precision Engineering and Manufacturing* [online]. 2015, **16**(1), p. 127-134. ISSN 2234-7593, eISSN 2005-4602. Available from: https://doi.org/ 10.1007/s12541-015-0016-2

[13] KIM, D. H., LEE, CH. M. A study on the development of a new conceptual automatic variable preload system for a spindle bearing. *The International Journal of Advanced Manufacturing Technology* [online]. 2013, **65**, p. 817-824. ISSN 0268-3768, eISSN 1433-3015. Available from: https://doi.org/10.1007/s00170-012-4219-8

[14] ZHANG, J., FANG, B., ZHU, Y., HONG, J. A comparative study and stiffness analysis of angular contact ball bearings under different preload mechanisms. *Mechanism and Machine Theory* [online]. 2017, **115**, p. 1-17. ISSN 0094-114X. Available from: https://doi.org/10.1016/j.mechmachtheory.2017.03.012

[15] LI, J., ZHU, Y., YAN, K., YAN, X., LIU, Y., HONG, J. Research on the axial stiffness softening and hardening characteristics of machine tool spindle system. *International Journal of Advanced Manufacturing Technology* [online]. 2018, **99**, p. 951-963. ISSN 0268-3768, eISSN 1433-3015. Available from: https://doi.org/10.1007/s00170-018-2456-1

[16] KACZOR, J., RACZYNSKI, A.The effect of preload of angular contact ball bearings on durability of bearing system. *Proceedings of the Institution of Mechanical Engineers, Part J: Journal of Engineering Tribology* [online]. 2015, **229**(6), p. 723-732. ISSN 1350-6501, eISSN 2041-305X. Available from: https://doi.org/10.1177/1350650114562485

[17] KACZOR, J., RACZYNSKI, A. The selection of preload in angular contact ball bearings according to the durability criterion. *Tribologia* [online]. 2018, **1**(277), p. 25-34. ISSN 0208-7774, eISSN 1732-422X. Available from: https://doi.org/10.5604/01.3001.0011.8284

[18] HARRIS, T. A. *Rolling bering analysis*. London: John Wiley and Sons, 2006. ISBN 9780849381676.

[19] KACZOR, J. Analysis of the influence of shaft load on the value of acceptable preload in a system of angular ball bearings. *Bimonthly Tribologia* [online]. 2020, **290**(2), p. 25-35. ISSN 0208-7774. Available from: https://doi.org/10.5604/01.3001.0014.3737

[20] JANG, G. H, KIM, D. K., HAN, J. H., KIM, C. S. Analysis of dynamic characteristics of a HDD spindle system supported by ball bearing due to temperature variation. *Microsystem Technologies* [online]. 2003, **9**, p. 243-249. ISSN 0946-7076, eISSN 1432-1858. Available from: https://doi.org/10.1007/s00542-002-0260-0

[21] KACZOR, J., RACZYNSKI, A. The selection of preload in angular contact ball bearings according to the criterion of moment of friction. *Tribologia* [online]. 2018, **1**(277), p. 35-44. ISSN 0208-7774, eISSN 1732-422X. Available from: https://doi.org/10.5604/01.3001.0011.8286

[22] KACZOR, J., RACZYNSKI, A. The influence of preload on the work of angular contact ball bearings. *Archive of Mechanical Engineering* [online]. 2016, **63**(3), p. 319-336. eISSN 2300-1895. Available from: https://doi.org/10.1515/meceng-2016-0018

[23] MOHAMMED, A., ABDALLAH, A. Effects of axial preloading of angular contact ball bearings on the dynamics of a grinding machine spindle system. *Journal of Materials Processing Technology* [online]. 2003, **136**(1-3), p. 48-59. ISSN 0924-0136. Available from: https://doi.org/10.1016/S0924-0136(02)00846-4

[24] RACZYNSKI, A. The calculation method of deep groove ball bearings durability with regard to clearance and shaft. *Scientific Problems of Machines Operation and Maintenance*. 1999, **34**(1), p. 111-120. ISSN 0137-5474.

[25] SKF catalog [online]. Available from: http://www.skf.com/group/products/bearings-units-housings/ball-bearings/angular-contact-ball-bearings/single-row-angular-contact-ball-bearings/single-row/index.html?designation=7212%20BEP

[26] LI, T., KOLAR, P., LI, X.-Y., WU, J. Research development of preload technology on angular contact ball bearing of high speed spindle. *International Journal of Precision Engineering and Manufacturing* [online]. 2020, **21**(6), p. 1163-1185. ISSN 2234-7593, eISSN 2005-4602. Available from: https://doi.org/10.1007/s12541-019-00289-5

[27] THAN, V., HUANG, J. H. Nonlinear thermal effects on high-speed spindle bearings subjected to preload. *Tribology International* [online]. 2015, **96**, p. 361-372. ISSN 0301-679X. Available from: https://doi.org/10.1016/j.triboint.2015.12.029

[28] TONG, V.-C., HWANG, J., SHIM, J., OH, J.-S., HONG, S.-W. Multi-objective optimization of machine tool spindle-bearing system. *International Journal of Precision Engineering and Manufacturing* [online]. 2020, **21**(10), p. 1885-1902. ISSN 2234-7593, eISSN 2005-4602. Available from: https://doi.org/10.1007/s12541-020-00389-7

[29] YAN, K.E., YAN, B., WANG, Y., HONG, J., ZHANG, J. Study on thermal induced preload of ball bearing with temperature compensation based on state observer approach. *The International Journal of Advanced Manufacturing Technology* [online]. 2016, **11**, p. 3029-3040. ISSN 0268-3768, eISSN 1433-3015. Available from: https://doi.org/10.1007/s00170-016-9469-4